Mol. Cryst. Liq. Cryst., Vol. 617: pp. 119–129, 2015

ISSN: 1542-1406 print/1563-5287 online
DOI: 10.1080/15421406.2015.1075841

Modified Driving Waveform for Stable High-Speed Address Discharge in AC PDP under High Xe Gas Mixture

JAE HYUN KIM,[1] HYUNG DAL PARK,[2] HYUN-JIN KIM,[3] AND HEUNG-SIK TAE[3,*]

[1]Radiation Instrumentation Research Division, Korea Atomic Energy Research Institute, Daejeon, Korea
[2]Department of Mechanical Equipment Development, Radiation Technology eXcellence (RTX), Daejeon, Korea
[3]School of Electronics Engineering, College of IT Engineering, Kyungpook National University, Daegu, Korea

For the fast and stable address under the high Xe gas condition of plasma display panels (PDPs), the weak and strong discharge characteristics in both surface-gap and plate-gap discharges were examined for two different Xe gas contents (7 and 20%). It is observed that it is very difficult to produce the strong plate-gap discharge required for the address discharge as the Xe gas content increases from 7 to 20%, thus requiring an additional voltage increase for the strong plate-gap discharge. Based on these experimental observations, the modified driving waveform, featuring being able to produce an intensified address discharge in the plate-gap discharge without a misfiring discharge in the surface-gap discharge, is proposed for the successful high speed address of the high Xe PDP.

Keywords High Xe content; surface-gap discharge; plate-gap discharge; high speed address; plasma display panel

1. Introduction

Various researches have been made to increase the luminous efficacy of the plasma display panels by increasing the partial pressure, *i.e.*, Xe contents in the ternary gas composition, He-Ne-Xe [1–5]. However, the increase in the Xe gas mixture inevitably causes an increase in the address discharge delay time as well as the breakdown voltage [6–8]. Moreover, the production of the address discharge is more difficult under the high Xe gas mixture conditions because the address discharge is produced between the plate-gaps where the electric field is uniform. Thus, improving the address discharge characteristics with a high Xe (>10%) gas mixture is very important and strongly depends on how the priming particles

*Address correspondence to Prof. Heung-Sik Tae, School of Electronics Engineering, College of IT Engineering, Kyungpook National University, Sangyuk-dong, Buk-gu, Daegu 702-701, Korea. E-mail: hstae@ee.knu.ac.kr

Color versions of one or more of the figures in the article can be found online at www.tandfonline.com/gmcl.

and electric field are used in the address discharge [7, 8]. As for the firing voltage with an increase in the Xe content, it is well known that the increase in the Xe concentration results in a reduced effective secondary electron emission coefficient and thus in an increase of the firing voltage [9–12]. Thus, although the driving methods using an electric field and priming particle have already been studied [13–16], the driving methods suitable for improving both the address capability and the stable driving under the high Xe (>20%) content conditions need to be studied further. Accordingly, this study proposes a modified driving waveform, featuring being able to produce an intensified address discharge in the plate-gap discharge without a misfiring discharge in the surface-gap discharge, for the successful high speed address of the high Xe (20%) PDP. The weak and strong discharge characteristics in both surface-gap and plate-gap discharges were examined for two different Xe gas contents (7 and 20%) conditions in the 42-in. HD grade PDP under the ADS driving scheme using the V_t closed curve analysis method and IR emission characteristics.

2. Experimental Methods

Figure 1 (a) shows a schematic diagram of a single pixel employed in the experiments. As shown in Fig. 1(a), the test panels used in this research were 42-inch HD ac-PDP modules with three electrodes, where X was the common electrode, Y was the scan electrode, and A was the address electrode. The discharge produced between the common (X) and scan (Y) electrodes is defined as a surface-gap discharge, whereas the discharge produced between

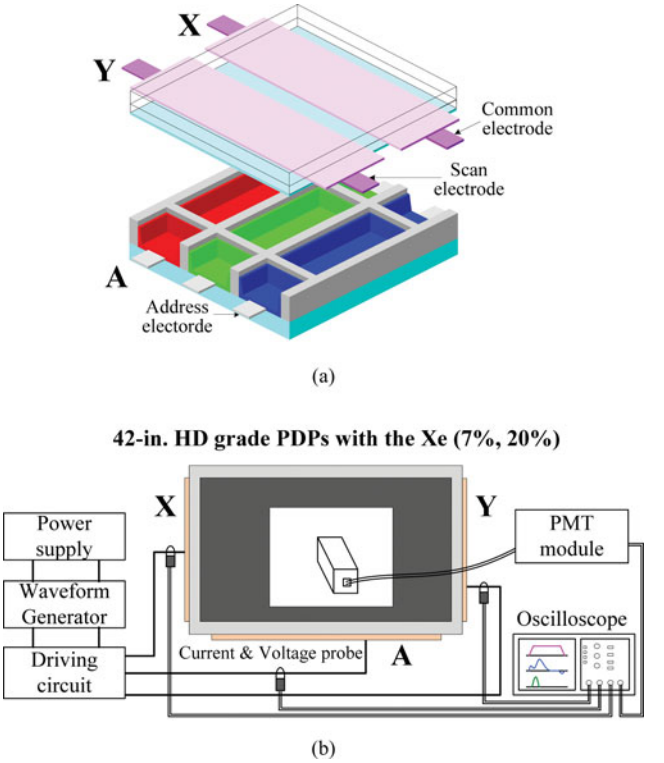

Figure 1. Schematic diagrams of structure of 42-in. test panel and experimental setup.

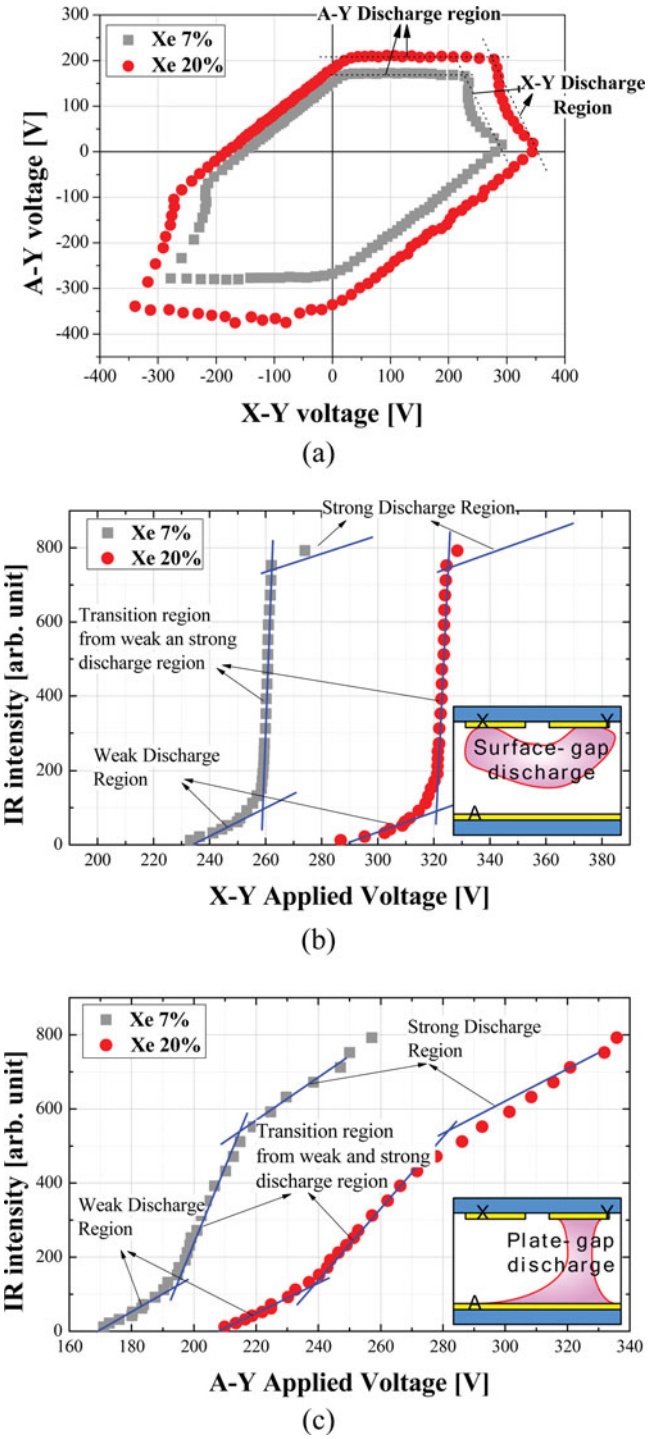

Figure 2. V_t closed curves and IR emission characteristics relative to Xe 7% and Xe 20% contents in test panels: (a) V_t closed curves without initial wall voltage, (b) IR intensity by X-Y applied voltage in X-Y discharge region, and (c) IR intensity by A-Y applied voltage in A-Y discharge region.

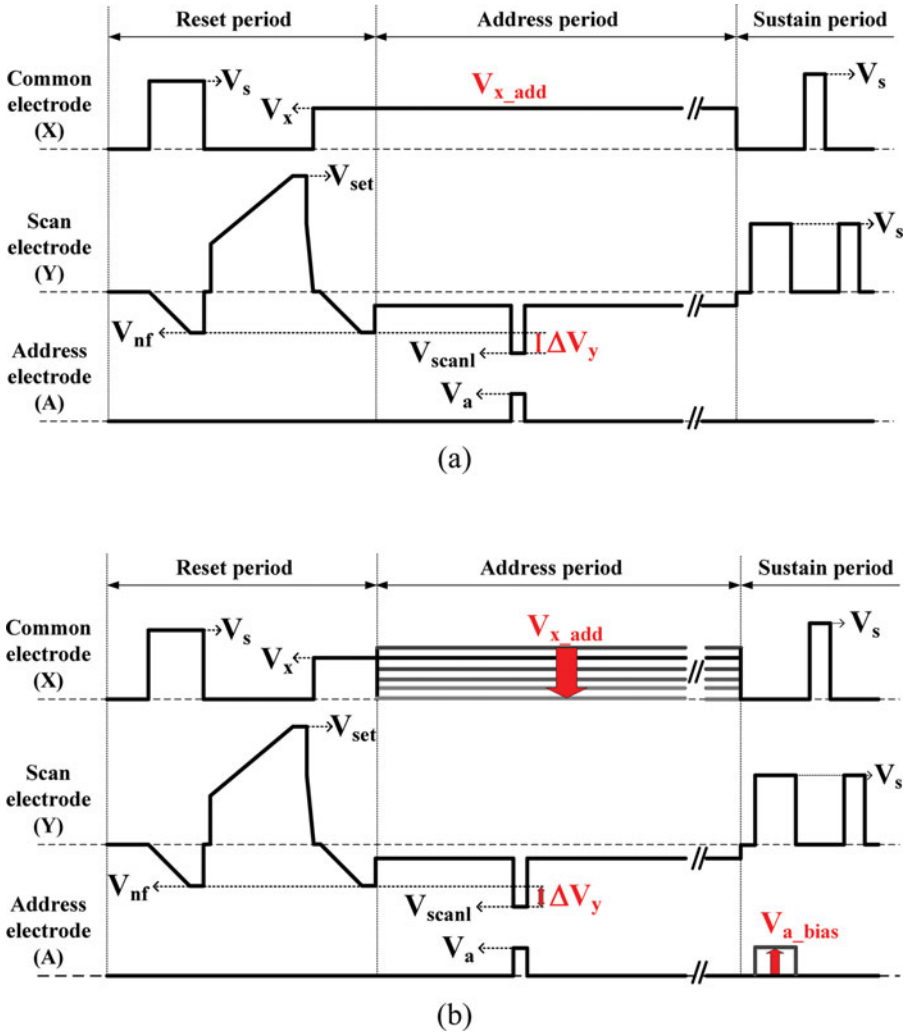

Figure 3. Schematic diagrams of driving waveforms: (a) conventional and (b) modified driving waveform in this study.

Table 1. Applied voltage conditions of conventional driving waveforms employed in this study

Test panel	Xe 7%	Xe 20%
V_s	175 V	210 V
V_{set}	280 V	340 V
V_{nf}	−140 V	−170 V
V_{scanl}	−160 V	−190 V
V_x	70 V	90 V
V_a	40 V	55 V

Table 2. Various applied voltage conditions employed in case study

Panel	Xe 7%					
Cases	a	b	c	d	e	
V_{x_add} [V]	85	75	50	25	0	
Panel	Xe 20%					
Cases	A	B	C	D	E	F
V_{x_add} [V]	125	100	75	50	25	0

the scan (Y) and address (A) electrodes is defined as a plate-gap discharge. The electric field intensity induced by the sustain-gap voltage is non-uniform, whereas the electric field intensity induced by the plate-gap voltage is relatively uniform. The gas mixture and pressure of test panel were Ne-He-Xe (7% and 20%) and 400 Torr, respectively. The cell conditions of test panels were exactly the same, except for the Xe content condition. Figure 1 (b) shows the schematic diagram of the experimental setup. As shown in Fig. 1 (b), the IR emission (823 nm) intensity measurement systems and 40-in. HD test panels with the Xe 7% and 20% were used in this experiment. A PMT (photomultiplier tube) and the waveform generator were used to measure the IR emission intensity, V_t closed curves, the address discharge delay time, and the driving margin in this study.

3. Results and Discussion

3.1. Weak and Strong Discharge Characteristics under Xe 7 and 20%

Figure 2 (a) shows the V_t closed curves of the surface-gap (X-Y) and plate-gap (A-Y) measured in the two different gas mixture conditions: Xe 7 and 20% without initial wall voltage. The firing voltage between the X-Y electrodes was increased by about 60 V, whereas the firing voltage between the A-Y electrodes was increased by about 35 V at a Xe 20% condition. Figure 2 (b) shows the change in the IR emission intensity as the voltage applied between the surface-gap (X-Y) is increased for the two different Xe gas conditions: 7 and 20%. Figure 2 (c) shows the changes in the IR emission intensity as the voltage applied between the plate-gap (A-Y) is increased for the two different Xe gas conditions: 7 and 20%. When comparing the transition of the IR emission intensity relative to the variation in the applied voltage in both surface-gap (Fig. 2 (b)) and plate-gap (Fig. 2 (c)) discharges, the IR emission intensity shows a abrupt increase for the surface-gap discharge was increased abruptly, whereas the IR emission intensity shows a slow increase for the plate-gap discharge. In particular, the IR emission intensity shows a very slow increase for the high Xe (20%) plate-gap discharge, meaning that it is not easy to produce the strong address discharge for accumulating the large amount of wall charges under the high (20%) Xe gas content.

3.2. Characteristics of Weak- Strong Discharge and ΔVy Driving Margin under Driving Conditions

Figure 3 (a) shows the schematic diagrams of commercial ADS driving waveform and Figure 3 (b) shows the proposed modified driving waveform for intensifying address

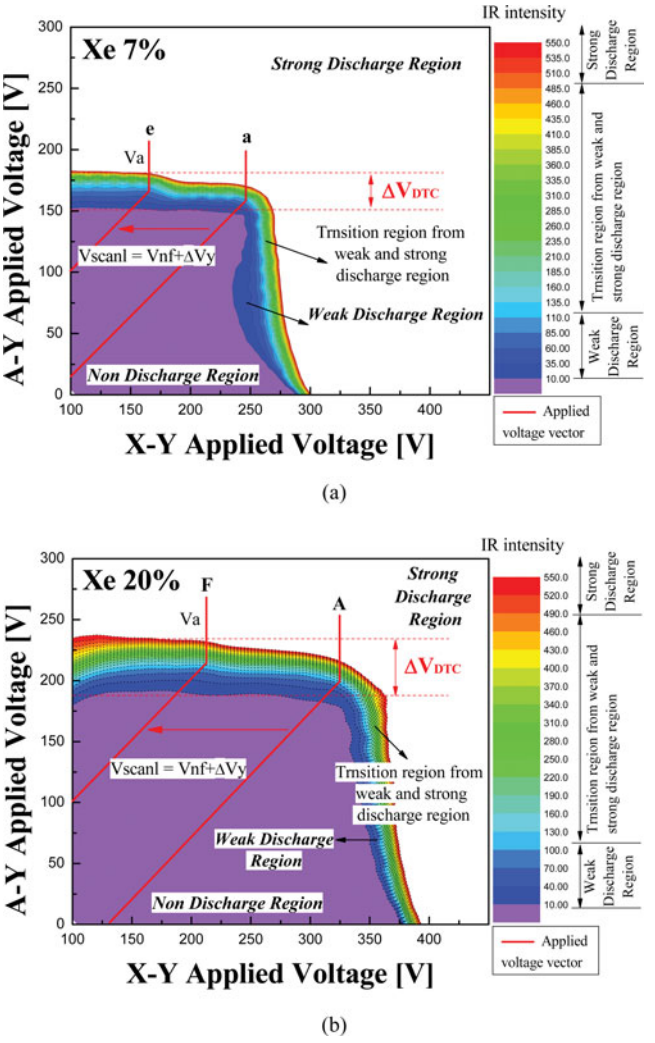

Figure 4. V_t closed curves and IR emission characteristics relative to Xe 7% and Xe 20% contents after reset discharge in test panels: (a) V_t closed curves and contours of same IR intensity, (b) IR intensity of V_{tAY} discharge region by various V_{x_add} , and (c) IR intensity of Xe 20% in A-Y discharge region.

discharge without a misfiring surface discharge under high Xe (20%) gas condition and the driving characteristics in this study. In the conventional driving waveform of Fig. 3 (a), where the voltage difference between the scan low voltage (V_{scanl}) and the negative falling voltage (V_{nf}) is defined as ΔV_y ($= V_{nf} - V_{scanl}$), and the magnitude of ΔV_y plays a role in intensifying between the A and Y electrodes *i.e.*, plate-gap discharge. The bias voltage of common electrode is defined as V_x, the magnitude of V_x plays a role in both suppressing the misfiring between the X and Y electrodes and facilitating the first sustain discharge after address period. In the modified driving waveform of Figure 3 (b), the V_{x_add} and ΔV_y were varied in order to intensify the address discharge between the

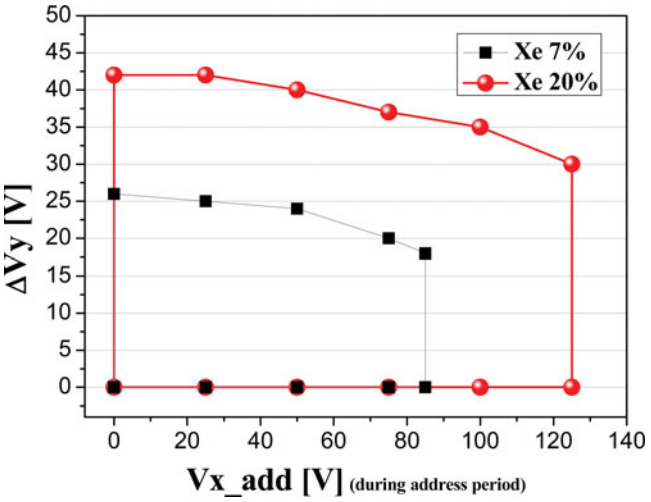

Figure 5. Comparison of ΔV_y dynamic driving voltage margin by V_{x_add}.

A-Y electrodes without a misfiring between the X-Y electrodes. Particularly, V_{a_add} was additionally applied with the first sustain pulse during sustain period in order to minimize side effect caused by modifying the ΔV_y and V_{x_add}. The detailed voltages of Fig. 3 (a) are shown Table 1. In Table 2, the values of V_{x_add} are changed from 85 to 0 [V] for Xe 7% and from 125 to 0 [V] for Xe 20% to analyze the address discharge characteristics during the address-period.

Figure 4 (a) and (b) show the V_t closed curves, same IR Intensity contour by increasing the applied voltage, and the applied voltage vectors ($V_{scanl} + V_a$) by decreasing V_{x_add} voltage after reset discharge relative to Xe 7% and Xe 20% contents during the address

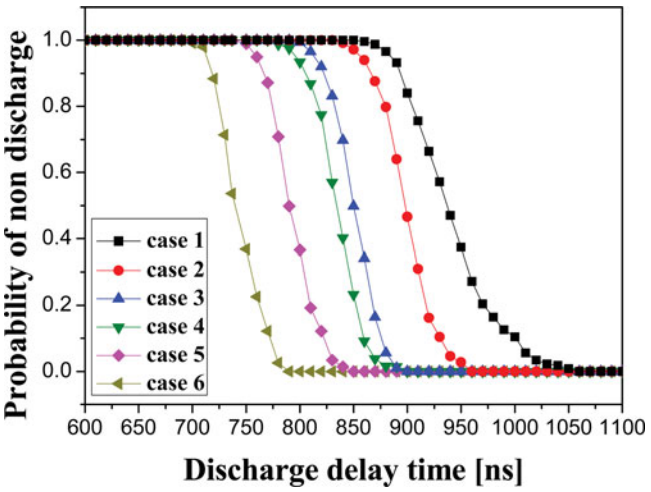

Figure 6. Probability of non discharge of Xe 20% test panel adopting cases (1 to 6) during address discharge.

Table 3. Applied voltage conditions of addressing case employed in case study

Cases	1	2	3	4	5	6
V_{x_add} [V]	125	100	75	50	25	0
V_{scanl} [V]	−190	−192.5	−195	−197.5	−200	−202.5
ΔV_y [V]	20	22.5	25	27.5	30	32.5
V_x [V]	90					
V_{nf} [V]	−170					
V_s [V]	210					
V_a [V]	55					

period in Fig. 3 and Table 2. As shown in Fig. 4 (a) and (b), the IR intensity contours were steadily increased by increasing the applied voltage and saturated at almost the same applied voltage. In Fig. 4 (a) and (b), the IR intensity contours are separated as three different regions; weak discharge region, transition region from weak and strong discharge region, strong discharge region. The ΔV_{DTC} shown in Fig. 4 is a voltage to enable the discharge transition from the weak and strong discharge, meaning that the additional application of ΔV_{DTC} can make the discharge. As shown in Figs. 4 (a) and (b), the weak discharge regions of the high Xe (20%) were larger than those of the low Xe (7%) after reset discharge, which means that the ΔV_y can be increased for High Xe (20%) contents. In particular, as shown in Figs. 4 (a) and (b), the weak discharge regions for the high Xe (20%) become larger as the A-Y voltage was increased and simultaneously the X-Y voltage ($= V_{x\_add}$) was decreased, meaning that the ΔV_y can be increased for high Xe contents.

Figure 5 shows the ΔV_y dynamic driving margin by various V_{x_add} of Xe (7 and 20%) contents without the misfiring discharge during the address period. As shown in Fig. 5, the ΔV_y dynamic driving margin is wider by about 15 V under the high Xe (20%) content because the high Xe content has the wider weak discharge region, as shown in Fig. 4 (b). Thus, the ΔV_y can be increased by reducing the V_{x_add} without any misfiring discharge in the sustain discharge.

3.3. Address Discharge Characteristics with Various ΔV_y and V_{x_add}

Figure 6 shows the probability of non discharge during the address discharge. As shown in Fig. 6, the address discharge delay times are reduced without misfiring discharge by increasing the ΔV_y based on the values in Table 3. Table 4 shows the address discharge delay time lags by various V_{x_add} in Xe 20% test panel. As shown in Table 4, the address discharge delay times (T_d) are reduced by about 200 ns without misfiring discharge by increasing ΔV_y and decreasing V_{x_add}. Therefore, high address speed under the high Xe

Table 4. Address discharge delay time lag in Xe 20% test panel

Cases	1	2	3	4	5	6
T_f [ns]	869	843	803	778	750	703
T_s [ns]	81	62	54	65	50	47
T_d [ns] ($= T_f + T_s$)	951	905	857	843	800	750

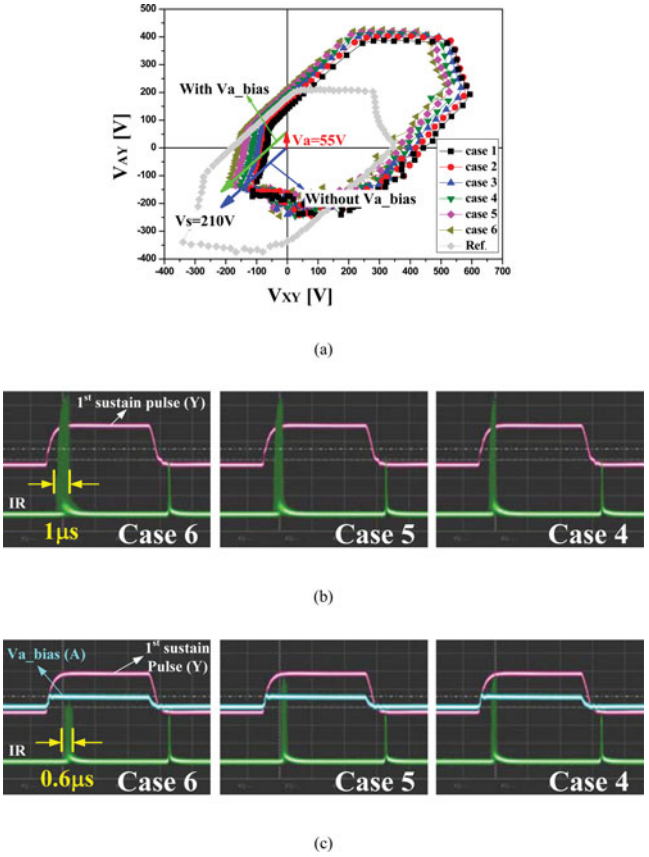

Figure 7. V_t closed curves after address discharge and IR emission of first sustain discharge: (a) V_t closed curves after address discharge under various address discharge condition, (b) first sustain discharge without V_{a_bias}, and (c) first sustain discharge with V_{a_bias}.

contents is successfully obtained through the proper control of ΔV_y and V_{x_add} based on the characterization of plate gap discharge and surface gap discharge as a function of Xe contents. The formative delay time in address discharge under high Xe gas content increases considerably because more intense electric field is required for producing discharge under high Xe gas content. In this sense, it is necessary to increase the electric field intensity between the A-Y electrodes for the case of adopting the high Xe content. However, the stability of the first sustain discharge is very sensitive to the application of the higher ΔV_y because increasing ΔV_y without adjusting the V_{x_add} can cause phosphor cathode-based discharge, thereby resulting in unstable discharge.

3.4. Sustain Discharge Characteristics with V_{a_bias}

Figure 7 shows V_t closed curves after the address discharge and the IR emission characteristics of first sustain discharge. As shown in Figure 7 (a), the V_t closed curves are shifted to the left after the address discharge when reducing the V_{x_add} and increasing the ΔV_y from case 1 to case 6. Without additional application of V_{a_bias} (= 55 V), the first sustain

discharges especially in cases 4∼6 are produced under the phosphor cathode discharge mode, as shown in the arrow of the V_t closed curved in Fig. 7 (a). Figure 7 (b) shows the unstable sustain discharges generated under the phosphor cathode discharge mode during the first sustain discharge, when adopting the lower V_{x_add} and higher ΔV_y, *i.e.*, cases 4∼6 during address period, and applying no V_{a_bias} (= 55 V) to the address electrode during the application of the first sustain pulse. However, the additional application of V_{a_bias} (= 55 V) to the address electrode during the application of the first sustain pulse shifted the first sustain discharge modes in cases 4∼6 from phosphor cathode discharge mode into MgO cathode discharge mode, as shown in the arrow of the V_t closed curve in Fig. 7 (a). As shown in Figure 7 (c), all the first sustain discharges in cases 4∼6 are produced stably when applying V_{a_bias} (= 55 V) to the address electrode during the application of the first sustain pulse, meaning that with help of V_{a_bias}, the fast addressing condition can be obtained in case 6 without unstable first sustain discharge under high Xe contents.

Conclusion

In this paper, the weak and strong discharge characteristics in both surface-gap and plate-gap discharges were examined for two different Xe gas contents (7 and 20%). Based on these experimental observations, the modified driving waveform, featuring being able to produce an intensified address discharge in the plate-gap discharge without a misfiring discharge in the surface-gap discharge, is proposed for the successful high speed address of the high Xe PDP. As a result, the address discharge delay time (T_d) is observed to be reduced by about 200 ns. Furthermore, the stable sustain discharge is obtained by applying the additional address bias during the application of first sustain pulse. Thus, it is expected that these modified driving waveforms and experimental results will help reduce the problem of unstable address discharge and sustain discharge in high Xe (> 20%) PDPs.

Funding

This research was supported by Basic Science Research Program through the National Research Foundation of Korea (NRF) funded by the Ministry of Education (2013R1A1A4A03008577).

References

[1] Weber, L. F. (2000). *in Proc. SID'04 Dig.*, p. 402.
[2] Park, K.-H., Tae, H.-S., Hur, M., & Heo, E. G. (2009). *IEEE Trans. Plasma Sci.*, *37*, 2061.
[3] Kim, T.-W., Kwon, S.-U., & Hwang, H.-J. (2003). *J. Korean Phys. Soc.*, *42*, S848.
[4] Chung, W. J., Shin, B. J., Kim, T. J., Bae, H. S., Seo, J. H., & Whang, K.-W. (2003). *IEEE Trans. Plasma Sci.*, *31*, 1038.
[5] Hayashi, D., Heusler, G., Hagelarr, G., & Kroesen, G. (2004). *J. Appl. Phys.*, *95*, 1656.
[6] Oversluizen, G., Itoh, K., Shiga, T., & Mikoshiba, S. (2008). *in Proc. SID'04 Dig.*, p. 374.
[7] Kim, J. S., Yang, J. H., Kim, T. J., & Whang, K. W. (2003). *IEEE Trans. Plasma Sci.*, *31*, 1083.
[8] Tachibana, K., Mizokami, K., Kosugi, N., & Sakai, T. (2003). *IEEE Trans. Plasma Sci.*, *31*, 68.
[9] Uchida, G., Uchida, S., Akiyama, T., Kajiyama, H., & Shinoda, T. (2010). *J. Appl. Phys.*, *107*, 103311.
[10] Ho, S., Uemura, N., Nobuki, S., Mori, S., Miyake, T., Suzuki, K., Mikami, Y., Shiiki, M., & Kubo, S. (2010). *IEEE Trans. Plasma Sci.*, *57*, 3377.
[11] Shiga, T., Saito, A., Tone, M., Mikoshiba, S., & Oversluizen, G. (2005). *J. Soc. Inf. Displ.*, *13*, 913.

[12] Park, H. D., Kim, J. H., Tae, H.-S., & Kim, B. S. (2013). *Mol. Cryst. Liq. Cryst.*, *585*, 25.
[13] Hayashi, D., Heusler, G., Hagelaar, G., & Kroesen, G. (2004). *J. Appl. Phys.*, *95*, 1656.
[14] Suraj, K. S., Sharma, S., & Dwivedi, H. K. (2010). *J. Phys.:Conf. Series*, *208*, 012115.
[15] Lee, W.-G., Shao, M. J., Gottschalk, R., Brown, M., & Compaan, A. D. (2002). *J. Appl. Phys.*, *92*, 682.
[16] Veronis, G., Inan, U. S., & Pasko, V. P. (2000). *IEEE Trans. Plasma Sci.*, *28*, 1271.